Presented at the 11th Annual CMAS Conference, Chapel Hill, NC, October 15-17, 2012

SENSITIVITY ANALYSIS OF INFLUENCING FACTORS ON $PM_{2.5}$ NITRATE SIMULATION

Hikari Shimadera[1,*], Hiroshi Hayami[1], Satoru Chatani[2], Yu Morino[3], Yasuaki Mori[4], Tazuko Morikawa[5], Kazuyo Yamaji[6], Toshimasa Ohara[3]

[1]Central Research Institute of Electric Power Industry, Abiko, Japan
[2]Toyota Central R&D Labs., Inc., Nagakute, Japan
[3]National Institute for Environmental Studies, Tsukuba, Japan
[4]Japan Weather Association, Tokyo, Japan
[5]Japan Automobile Research Institute, Tsukuba, Japan
[6]Japan Agency for Marine-Earth Science and Technology, Yokohama, Japan

1. INTRODUCTION

Fine particulate matter ($PM_{2.5}$) has been of increasing concern because of its adverse effects on human health. The Ministry of the Environment of Japan introduced an air quality standard for $PM_{2.5}$ in 2009. Although $PM_{2.5}$ concentrations have decreased in recent years in Japan, the standard for $PM_{2.5}$ is not attained in most urban areas in Japan. Although air quality models (AQMs) with reasonable accuracy are essential tools to develop and evaluate measures to attain the standard, current air quality models cannot adequately simulate atmospheric mass concentrations of $PM_{2.5}$ and its components in the Kanto region of Japan (Morino et al., 2010).

This study focused on secondary inorganic aerosols among major $PM_{2.5}$ components. Air quality simulations were conducted in the Kanto region in winter 2010 and summer 2011 by using the Community Multiscale Air Quality modeling system (CMAQ) (Byun and Schere, 2006) with several configurations. Because large discrepancies occurred between observed and simulated NO_3^- concentrations as described in section 3, sensitivity analyses were conducted in order to investigate factors influencing the model performance for NO_3^- simulation.

2. METHODOLOGY

Fig. 1 shows modeling domains and locations of observation sites for $PM_{2.5}$ and its components. The horizontal domains consist of three domains from domain 1 (D1), covering a wide area of East Asia, to domain 3 (D3), covering most of the Kanto region. The horizontal resolutions and the number of grid cells are 64, 16 and 4 km, and 96 × 80, 56 × 56 and 56 × 56 for D1, domain 2 (D2) and D3, respectively. The vertical layers consist of 30 sigma-pressure coordinated layers from the surface to 100 hPa with the middle height of the first layer being approximately 28 m.

Meteorological fields were produced using the Weather Research and Forecasting model (WRF) (Skamarock and Klemp, 2008) version 3.2.1 driven by the final analysis data and the high-resolution global sea surface temperature analysis data of the National Centers for Environmental Prediction. WRF was configured with the Kain-Fritsch cumulus parameterization in D1 and D2, the Asymmetrical Convective Model version 2 (ACM2) for the planetary boundary layer parameterization, the WRF single-moment 5-class microphysics scheme, the Pleim-Xiu land surface model, the rapid radiative transfer model for the longwave radiation and the Dudhia scheme for the shortwave radiation. Grid nudging was applied to wind, temperature and humidity in D1 and D2

Emission data were produced according to the method described by Chatani et al. (2011). Anthropogenic emissions in D1 were derived from the INTEX-B Asian emission inventory for SO_2, NO_X, CO, PM and volatile organic compounds (VOC), and from the regional emission inventory in Asia (REAS) for NH_3. Anthropogenic emissions in D2 and D3 were estimated with the Japan Auto-Oil Program (JATOP) vehicle emission estimate model and the Georeference-Based Emission Activity Modeling System (G-BEAMS). Ship emissions were derived from emission inventories developed by the National Maritime Research Institute (NMRI) and the Ocean Policy Research Foundation (OPRF). Biogenic VOC emissions were estimated with the Model of Emissions of Gases and Aerosols from Nature (MEGAN) version 2.04.

Table 1 summarizes five kinds of CMAQ configurations (M0-M4). Initial and boundary

*Corresponding author: Hikari Shimadera, Central Research Institute of Electric Power Industry, Abiko 1646, Abiko, Chiba 270-1194, Japan; e-mail: simadera@criepi.denken.or.jp

Table 1 CMAQ configurations.

	M0	M1	M2	M3	M4
AQM	CMAQ v4.7.1	CMAQ v4.7.1	CMAQ v4.6	CMAQ v4.7.1	CMAQ v5.0
Domain	D1, D2, D3	D3	D3	D1, D2, D3	D3
Horizontal advection	Yamartino	Yamartino	Yamartino	PPM	Yamartino
Vertical advection	Yamartino	Yamartino	Yamartino	PPM	WRF
Horizontal diffusion	Multiscale	Multiscale	Multiscale	Multiscale	Multiscale
Vertical diffusion	ACM2	ACM2	ACM2	ACM2	ACM2
Photolysis rate	Lookup table	On-line	Lookup table	On-line	On-line
Gas phase	SAPRC99 (EBI)	SAPRC99 (EBI)	SAPRC99 (ROS3)	SAPRC99 (EBI)	SAPRC99 (EBI)
Aerosol phase	AERO5	AERO5	AERO4	AERO5	AERO5
Cloud phase	ACM	ACM	RADM	ACM	ACM

concentrations for D1 were obtained from the Model for Ozone and Related Chemical Tracers version 4 (MOZART-4). CMAQ simulations were conducted for periods from November 15 to December 5, 2010 and July 11 to 31, 2011, with the first seven days being initial spin-up periods. M0 is the baseline simulation case in this study. Results of M0 were used for boundary concentrations for M1, M2 and M5, and are compared with the observation data in the next section.

3. MODEL EVALUATION

Fig. 2 shows observed and M0-simulated mean concentrations of $PM_{2.5}$ and its components including organic aerosol (OA), elemental carbon (EC), SO_4^{2-}, NO_3^- and NH_4^+, and gaseous HNO_3 and NH_3 at the observation sites in winter 2010. The M0-simulated mean concentrations of $PM_{2.5}$, EC except at Kisai, and SO_4^{2-} approximately agreed with the observations. However, the model clearly underestimated OA concentrations at the observation sites, and overestimated NO_3^-, HNO_3 and NH_3 concentrations at Kisai.

Fig. 3 shows observed and M0-simulated mean concentrations of $PM_{2.5}$ and its components, and gaseous HNO_3 and NH_3 at the observation sites in summer 2011. The M0-simulated mean concentrations of $PM_{2.5}$, EC, SO_4^{2-} and HNO_3 concentrations approximately agreed with the observations. However, the model clearly underestimated OA concentrations, and clearly overestimated NO_3^- and NH_3 concentrations. The overestimation of NO_3^- concentration is likely attributed to overestimation of NH_4NO_3 production.

The agreement of mean $PM_{2.5}$ concentrations between the observation and simulation in this study does not indicate a good model performance because it is due to compensation of the overestimations and underestimations of $PM_{2.5}$ components. Results of sensitivity analyses to

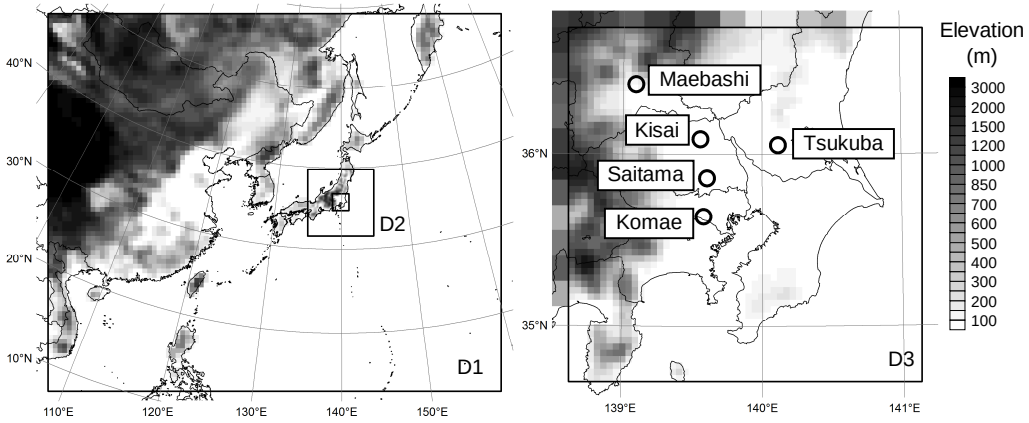

Fig. 1. Modeling domains and locations of observation sites for PM2.5 and its components.

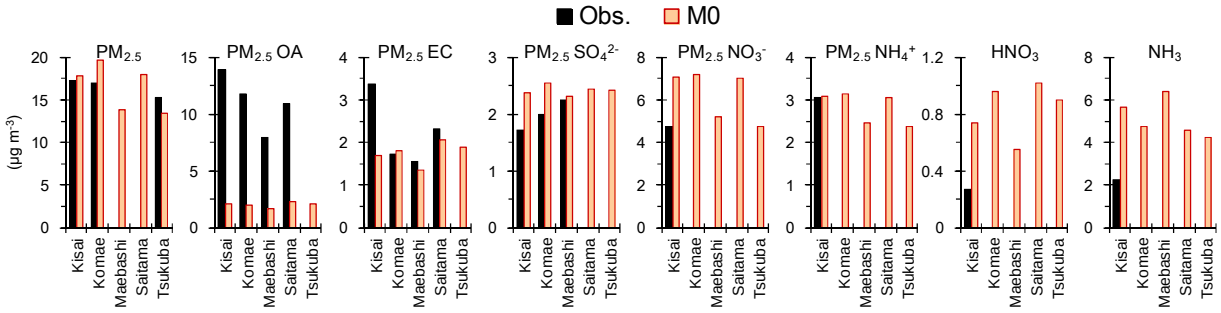

Fig. 2 Comparisons of observed and M0-simulated mean concentrations in winter 2010.

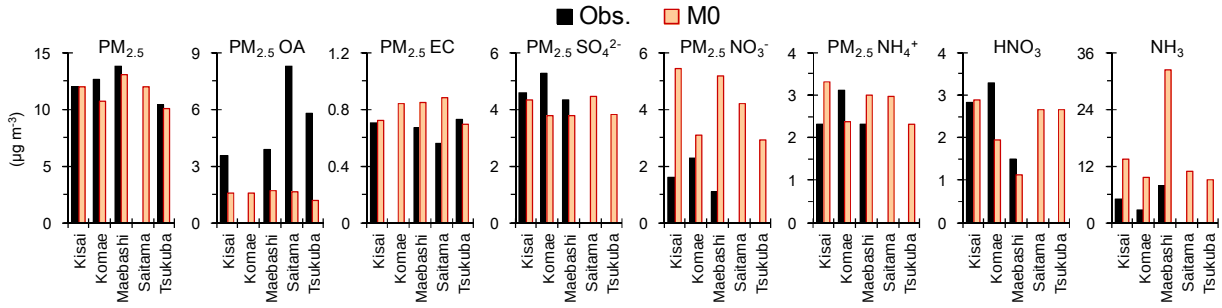

Fig. 3 Comparisons of observed and M0-simulated mean concentrations in summer 2011.

investigate influencing factors on the overestimation of NO_3^- are presented in the next section.

4. SENSITIVITY ANALYSES

4.1 Different CMAQ Configurations

For simplification, results of sensitivity analyses were compared by percentage differences of mean concentrations from each baseline cases in land areas with an elevation less than 200 m in D3 (target area) during November 22 to December 5, 2010 and July 18 to 31, 2011.

Fig. 4 shows comparisons of results of M0-M4. Because of common meteorological, emission and boundary concentration data, temporal variation patterns of simulated concentrations at the observation sites were very similar to each other (not shown). Although the results of M1 and M3, which are CMAQ version 4.7.1 (the same version as M0), were relatively similar to those of M0, it was indicated that on-line calculation of photolysis rate slightly reduced NO_3^- in Kanto in summer. The results of M2 were the most different from the others due to various different configurations. M4, which is CMAQ version 5.0 in which minimum eddy diffusivity reduced from 0.5 to 0.01 m^2 s^{-1}, predicted higher ground-level concentrations under stable conditions during nighttime.

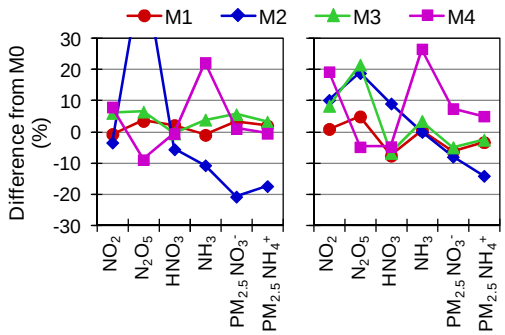

Fig. 4 Percentage differences of mean concentrations from M0 in the target area in winter 2010 (left) and summer 2011 (right) for M1-M4.

4.2 Temperature and Relative Humidity

NH_4NO_3 is a semi volatile compound can exist in gaseous and particulate phase mainly depending on temperature and relative humidity.

Sensitivity analyses of temperature and relative humidity were conducted in D3 by M0. In sensitivity cases, temperature or relative humidity used in aerosol module was uniformly changed by ±2 K (T+2, T-2) or by ±10% (RH+10, RH-10). Fig. 5 shows results of the sensitivity analyses. In higher temperature and lower relative humidity, NH_4NO_3 easily shifts to the gas phase. Note that temperature and relative humidity affect not only gas/aerosol partitioning in aerosol module but other processes such as heterogeneous reaction

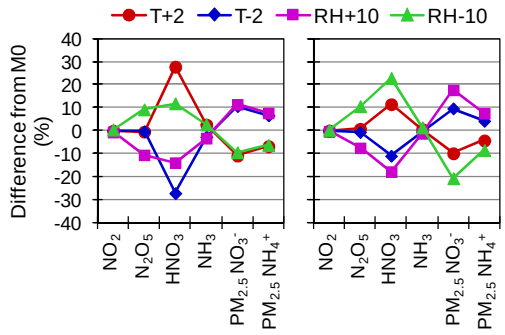

Fig. 5 Percentage differences of mean concentrations from M0 in the target area in winter 2010 (left) and summer 2011 (right) for sensitivity analyses of temperature and relative humidity.

The results indicate even errors of temperature and humidity that sometimes occur can cause over- or underestimation of NO_3^-.

4.3 NO_X Emission

Sensitivity analysis of NO_X emission was conducted in D3 by M1. In sensitivity cases, NO_X emission was uniformly changed by from -40% to +40% (E-40, E-20, E+20, E+40). Fig. 6 shows results of the sensitivity analysis. Although the sensitivity of NO_X emission to NO_2 concentration was large, the sensitivity to NO_3^- concentration was relatively small. Because uncertainty in total NO_X emission in Japan is probably smaller than 40%, improvement of NO_X emission is unlikely to be a key factor for improvement of NO_3^- simulation.

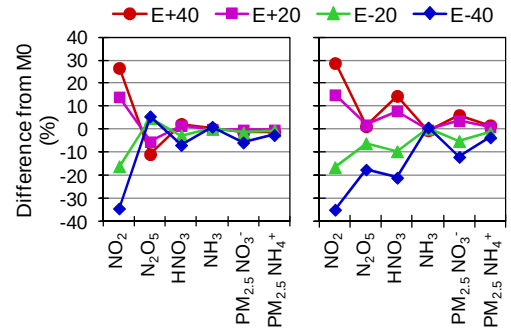

Fig. 6 Percentage differences of mean concentrations from M1 in the target area in winter 2010 (left) and summer 2011 (right) for sensitivity analysis of NO_X emission.

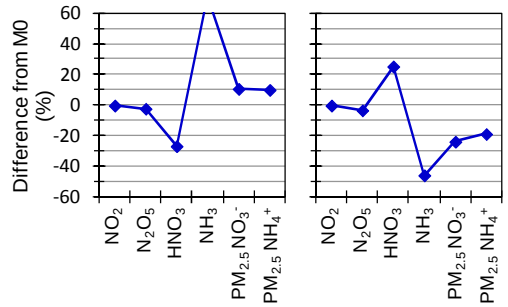

Fig. 7 Percentage differences of mean concentrations from M0 in the target area in winter 2010 (left) and summer 2011 (right) for sensitivity analysis of seasonal variation of NH_3 emission.

4.4 Seasonal variation of NH_3 Emission

Sensitivity analysis of NH_3 emission was conducted in D2 to D3 by M0. For sensitivity runs, a seasonal variation of NH_3 emission was estimated according to processes for N_2O emission estimate in Japan (National Institute for Environmental Studies, 2012). Using the seasonal variation, total emission in D3 increased by 52% in winter and decreased by 42% in summer. Fig. 7 shows results of the sensitivity analysis. The change of NH_3 emission directly affected NH_3 concentration, and substantially affected formation of NH_4NO_3. In Japan, observation data of NH_3 concentration are not sufficiently available for model evaluation. Therefore uncertainty in NH_3 emission estimate is probably large and improvement of NH_3 emission may be one of the key factors for improvement of NO_3^- simulation.

4.5 HNO_3 and NH_3 Dry Depositions

Gaseous HNO_3 and NH_3 are efficiently removed from the atmosphere through dry deposition. While mean dry deposition velocities of HNO_3 and NH_3 in the target area in daytime ranged from 1 to 5 cm s^{-1} in M2, Neuman et al. (2004) estimated much higher dry deposition velocities of HNO_3 in daytime (8 to 26 cm s^{-1}).

Sensitivity analysis of HNO_3 and NH_3 dry deposition velocities was conducted in D3 by M2.

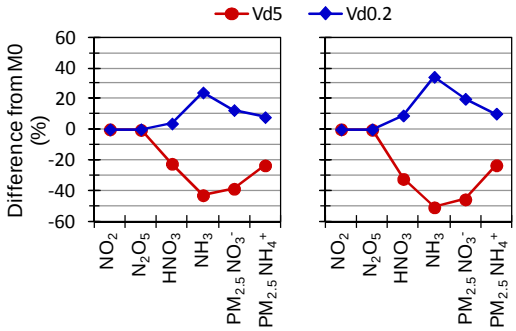

Fig. 8 Percentage differences of mean concentrations from M2 in the target area in winter 2010 (left) and summer 2011 (right) for sensitivity analysis of HNO_3 and NH_3 dry deposition velocities.

In sensitivity cases, the dry deposition velocities were uniformly multiplied by 5 (Vd5) and 0.2 (Vd0.2). Fig. 8 shows results of the sensitivity analysis. Higher dry deposition velocities substantially decrease concentrations of HNO_3 and NH_3, and consequently NH_4NO_3. Because of difficulty in evaluation of dry deposition process, uncertainty in simulated deposition velocity is probably large. Therefore, HNO_3 and NH_3 dry deposition velocities can be one of the key factors for improvement of NO_3^- simulation.

4.6 N_2O_5 Heterogeneous Reaction

Sensitivity analysis of N_2O_5 heterogeneous reaction was conducted in D3 by M0. In sensitivity cases, the heterogeneous reaction probability (Γ_{N2O5}) was set to 0 (no reaction; Γ0) and 0.1 (upper limit; Γ0.1). In addition, sensitivity runs using parameterization methods of the probability used in AERO3 (Γae3) and AERO4 (Γae4), which are older aerosol modules of CMAQ, were conducted. Fig. 9 shows results of the sensitivity analysis. NO_3^- concentrations in Γ0 case were lower by about 20% in winter and 10 % in summer than those in M0. These rates indicate the

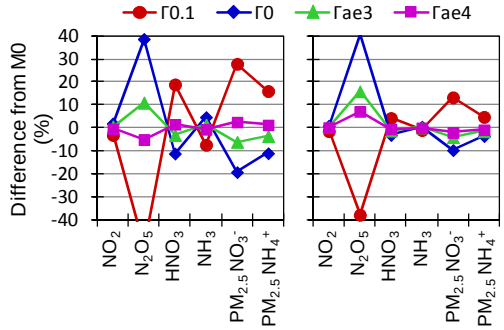

Fig. 9 Percentage differences of mean concentrations from M0 in the target area in winter 2010 (left) and summer 2011 (right) for sensitivity analysis of N_2O_5 heterogeneous reaction.

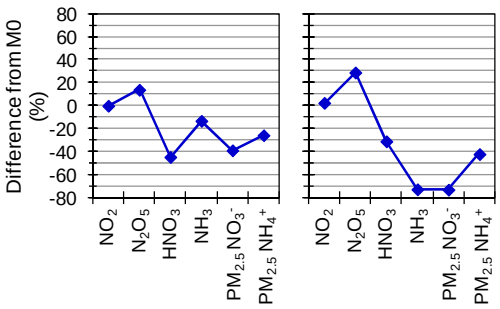

Fig. 10 Percentage differences of mean concentrations from M0 in the target area in winter 2010 (left) and summer 2011 (right) for ModMulti case.

contribution of NO_3^- production through the heterogeneous reaction in M0. Therefore, uncertainty in the heterogeneous reaction is not a dominant cause of the overestimation of NO_3^- concentration. However, modification of the Γ_{N2O5} parameterization method can slightly mitigate the overestimation.

4.7 Modification of Multiple Factors

Multiple factors that can mitigate the overestimation of NO_3^- concentration were simultaneously applied to M0 (ModMulti). ModMulti case is different from M0 in using on-line calculation of photolysis rate, the modified seasonal variation of NH_3 emission, fivefold dry deposition velocities of HNO_3 and NH_3, and the Γ_{N2O5} parameterization method of AERO3. Fig. 10 shows results of the sensitivity analysis. The results showed substantial decrease of NH_3 and NO_3^- concentrations, particularly in summer.

Figs. 11 and 12 show observed, M0- and ModMulti-simulated mean concentrations of $PM_{2.5}$ and its ionic components, and gaseous HNO_3 and NH_3 at the observation sites in winter 2010 and summer 2011, respectively. In winter, the difference between M0- and ModMulti-simulated NH_3 concentrations was relatively small because the effect of higher dry deposition velocities compensated the effect of larger NH_3 emission. In summer, NH_3 concentrations of ModMulti case were substantially lower than those of M0 mainly because of the combined effect of higher dry deposition velocities and smaller NH_3 emission in summer. Changes in HNO_3 and NH_3 concentrations affected formation of NH_4NO_3. $PM_{2.5}$ concentrations of ModMulti case were lower than those of M0 because of lower concentrations of ionic components, particularly NO_3^-. Consequently, NO_3^- concentrations of ModMulti case were closer to the observations than those of M0. Using fivefold dry deposition velocities may be unrealistic and has no theoretical support. However, the results indicate that such drastic modification may be required to improve the model performance for NO_3^- concentration.

5. SUMMARY

Air quality simulations using CMAQ were conducted in the Kanto region of Japan in winter 2010 and summer 2011. Although the model approximately reproduced EC and SO_4^{2-} concentrations, it clearly underestimated OA and clearly overestimated NO_3^- and NH_3 concentrations.

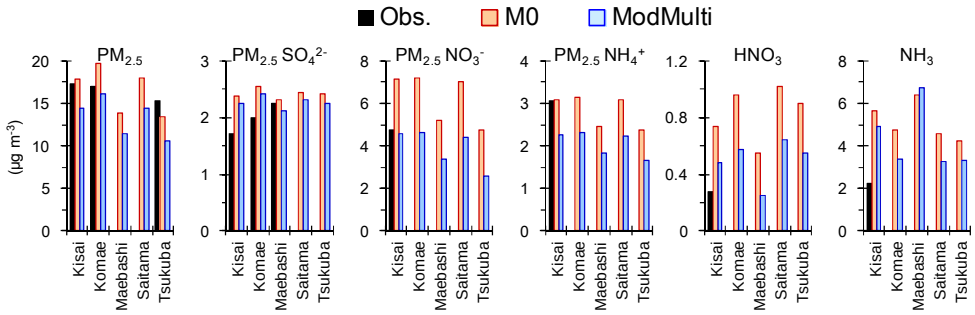

Fig. 11 Comparisons of observed, M0- and ModMulti-simulated mean concentrations in winter 2010.

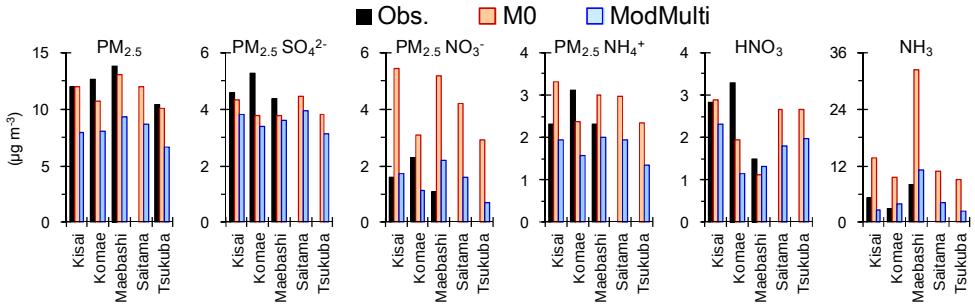

Fig. 12 Comparisons of observed, M0- and ModMulti-simulated mean concentrations in summer 2011.

Sensitivity analyses were conducted in order to investigate factors influencing the model performance for NO_3^- simulation. The investigated factors include several CMAQ configurations, temperature and relative humidity, NO_X emission, NH_3 emission, HNO_3 and NH_3 dry depositions, and N_2O_5 heterogeneous reaction. The analyses showed considerable sensitivities of NH_3 emission and HNO_3 and NH_3 dry depositions to NO_3^- concentration. Because there still remain large uncertainties in estimates of NH_3 emission and HNO_3 and NH_3 dry depositions, these may be key factors to improve the model performance for NO_3^- simulation.

6. ACKNOWLEDGEMENTS

This research was supported by the Environment Research and Technology Development Fund (C-1001) of the Ministry of the Environment, Japan. We are grateful to NMRI and OPRF for providing the ship emission inventories.

7. REFERENCES

Byun, D. and K. L. Schere. 2006: Review of the governing equations, computational algorithms, and other components of the models-3 community multiscale air quality (CMAQ) modeling system. *Appl. Mech. Rev.*, **59**, 51-76,

Chatani, S., T. Morikawa, S. Nakatsuka, S. Matsunaga, and H. Minoura, 2011: Development of a framework for a high-resolution, three-dimensional regional air quality simulation and its application to predicting future air quality over Japan. *Atmos. Environ.*, **45**, 1383-1393.

Morino, Y., S. Chatani, H. Hayami, K. Sasaki, Y. Mori, T. Morikawa, T. Ohara, S. Hasegawa, and S. Kobayashi, 2010: Inter-comparison of chemical transport models and evaluation of model performance for O3 and PM2.5 prediction - Case study in the Kanto area in summer 2007. *J. Japan Soc. Atmos. Environ.*, **45**, 212-226 (in Japanese).

National Institute for Environmental Studies, 2012: National Greenhouse Gas Inventory Report of JAPAN.

Neuman, J. A., D. D. Parrish, T. B. Ryerson, C. A. Brock, C. Wiedinmyer, G. J. Frost, J. S. Holloway, and F. C. Fehsenfeld. 2004: Nitric acid loss rates measured in power plant plumes. *J. Geophys. Res.*, **109**, D23304.

Skamarock, W. C. and J. B. Klemp. 2008: A time-split nonhydrostatic atmospheric model for weather research and forecasting applications. *J. Comput. Phys.*, **227**, 3465-3485.